SUNSAT baseplate design, finite element analysis and manufacturing

K. van der Westhuizen,[1] **A.H. Basson**[2] **and H.R. Schuster**[3]
(Received December 1994; Final version May 1995)

Abstract

The design, finite element analysis, and testing of the aluminium baseplate and payload adapter assembly of Sunsat are described. The primary design requirements for the baseplate are that the cantilevered modes' lowest natural frequency for the complete satellite, mounted rigidly on the payload adapter assembly, must exceed 70 Hz, and that 10 g accelerations must be sustained. A finite element model of the payload adapter, baseplate, and lowest tray, with the remainder of the satellite represented by a concentrated mass, was used to optimize the rib configuration in the baseplate. In a subsequent finite element analysis of the complete satellite structure, the first two lateral bending modes were found to be 70.0 and 70.5 Hz. Modal survey tests gave corresponding measured frequencies of 65 and 68 Hz. Mathematical model correlation and the results obtained thereby are described. Strength design requirements, analysis and testing procedures for design verification are outlined.

Introduction

This paper describes the mechanical design of the baseplate and mounting ring of SUNSAT. The use of Finite Element Modeling in the optimization and analysis of the baseplate, and the tests performed to confirm compliance with the design requirements, are discussed. The manufacturing of the baseplate by numerically controlled machining is discussed briefly, with particular reference to a novel approach to generation of cutter path programs.

SUNSAT is an acronym for Stellenbosch University Satellite. The primary motivation behind SUNSAT is to increase engineering design opportunities for graduate students, help promote interest in technology through school interaction programs, and increase industrial and international interaction. The current SUNSAT development team consists of approximately 30 post-graduate students (mostly in electronic engineering), and academic and technical staff members of the University of Stellenbosch. SUNSAT has a weight of 60 kg and a cubic size of 450 mm. It is designed to carry an amateur radio transponder, a store-and-forward communication system, and a three-colour imaging system with a resolution of 15 m. Its planned functional lifetime in orbit is approximately 4 years.

The Department of Electrical and Electronic Engineering at the University of Stellenbosch started the SUNSAT micro-satellite project in 1989. Studies of the Department's capabilities and other programmes at the universities of Surrey and Berlin led to the January 1992 baseline design compatible with ARIANE launch requirements. In 1994, NASA expressed interest in launching SUNSAT in the same mission as the Danish Oersted magnetic research satellite, both as secondary payloads on the Argos/P91-1 Delta II mission in October 1996. In exchange, SUNSAT will provide data gathered by a precision GPS receiver (that NASA will supply) and the mounting of a set of laser retro-reflectors on SUNSAT. The proposed orbit is near-polar with an inclination of 96° and an altitude varying from 450 km to 850 km.[1]

Review of previous work

Thorough surveys of other international activities involving small spacecraft have been given by Horais,[2] and Hatleid & Sterling.[3] Only a brief summary of relevant aspects will be given here.

The University of Surrey has pioneered micro-satellite technologies, beginning with its UoSAT programme in 1979. Surrey's first experimental micro-satellites (UoSAT-1 and 2) were launched free-of-charge as 'piggy-back' payloads through a collaborative arrangement with NASA on DELTA rockets in 1981 and 1984, respectively. Since then, a further eight low cost, yet fairly sophisticated, micro-satellites have been placed in low Earth orbit for a variety of customers using the ARIANE Auxiliary Payload Adapter.

UoSAT-1 and 2 both used a rather conventional structure – a framework 'skeleton' onto which modules containing the various electronic subsystems and payloads were mounted. However, the need to accommodate a variety of payload customers within a standard launcher envelope, coupled with increased demands on packing density, economy of manufacture and ease of fabrication, led to the development of a modular design of a multi-mission micro-satellite platform. This structure is based on a series of module trays that house the electronic circuits and themselves form the mechanical structure, onto which solar arrays are mounted.[4]

A companion paper [5] outlines the design of the overall mechanical configuration of SUNSAT, which also uses the concept of module trays, similar to the later satellites

[1] Graduate student

[2] Associate Professor (Member)

[3] Graduate student, Department of Mechanical Engineering, University of Stellenbosch, Stellenbosch, 7600 South Africa

produced by Surrey. SUNSAT's module trays are stacked on top of one another and clamped between the top plate and baseplate by four bolts on the corners (Figure 1).

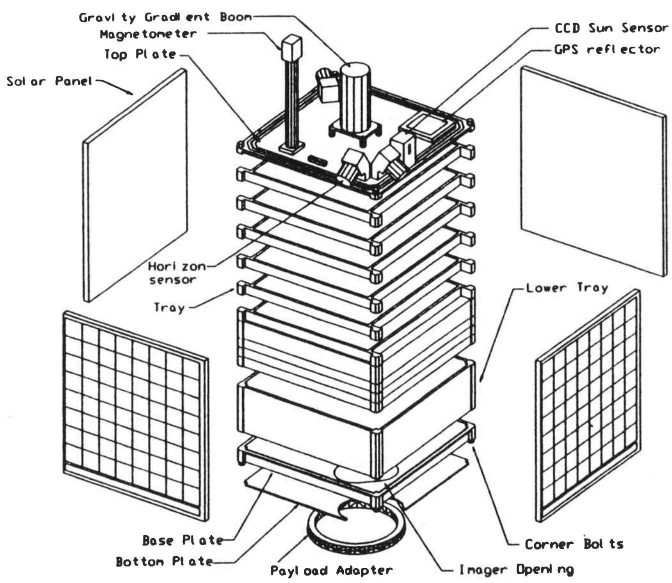

Figure 1 SUNSAT general structural configuration (exploded view)

No detailed information is available about the baseplates of previous micro-satellites.

Lower assembly configuration

The payload adapter assembly (PAA) and payload adapter fitting (PAF) are used to attach the satellite to the launch vehicle. Before launch, the PAA is attached to the bottom of the baseplate. The PAA mates with the PAF which is, in turn, fixed to the launch vehicle.

The Delta launcher interface separation mechanism and overall dimensions are supplied by the launcher company, McDonnell Douglas Aerospace (MDA).[6] The launcher company provides the PAF on the DELTA rocket, the clamp band and the separation springs, whilst the PAA is designed and supplied by the SUNSAT team. The PAA has to be a separate component and not form part of the base of the satellite because the PAA has to be assembled with the PAF by installing the clamp band, separation springs and switches, before attaching the PAA to the baseplate. The integration of the PAA and PAF is impractical when the PAA is an integral part of the baseplate. The assembled PAA and PAF are attached to SUNSAT before the PAF is integrated with the launch vehicle. Figure 2 shows the separation mechanism.

Design requirements

The design of the baseplate is dominated by functional requirements, mission requirements, financial constraints, and, in particular, launch requirements for the complete satellite.

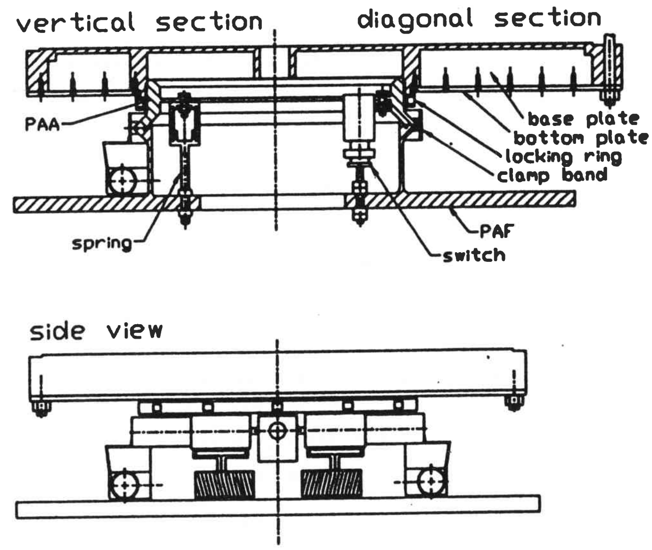

Figure 2 SUNSAT separation mechanism and baseplate assembly

Baseplate and PAA functional requirements

The main function of the baseplate is to support the lower satellite tray and all the components bolted to the top of the baseplate (imager, battery cases and reaction wheels) and to transmit forces from the lower tray and corner bolts to the PAA. The function of the PAA is to connect the baseplate to the PAF (that is attached to the launch vehicle) and make provision for the placement of the separation switches and springs, as well as the separation switch electrical connection to the baseplate.[6]

Mission requirements

The mission requirements result from the required field of view for the look-down imager. The large opening near the one corner of the baseplate for the imager to look down through (shown in Figure 1) has a significant effect on the structural design. The imager design and mission requirements determined the location and size of the opening. Changes to the imager opening would only have been considered if the stiffness, mass, and dimensional limits could not be satisfied.

Other design requirements, associated with operation in outer space, that eventually did not have a significant influence on the design, but still had to be considered, are the following (more general discussions of these requirements are given by Griffen & French [7]):

1. Enclosed volumes have to be adequately vented to avoid the build up of pressure differentials due to the rapid reduction in ambient pressure during the launch.

2. Materials that outgas (emit vapour) should not be used, because the vapour may condense on the imager optics and other sensors.

3. A minimum wall thickness (typically 2 mm for aluminium) must be maintained to protect internal electronics from degradation due to total radiation dose and malfunctions induced by so-called single-event upsets.

4. The structure must not be susceptible to corrosion in orbit (due to high energy atomic oxygen) or in the atmosphere.

Financial constraints

Financial constraints (imposed by the limited funding available) introduced some additional design requirements that had a significant influence on the baseplate design, particularly relating to the manufacturing and testing of the satellite.

The manufacturing requirements were that the baseplate and PAA had to be preferably manufactured in the university's workshop and that materials that are readily available, at moderate prices, had to be used. Conventional lathes, milling machines and a 3-axis NC machine are available in the workshop. Manufacturing in composite materials could not be accommodated in this workshop at the time that the baseplate was produced.

The costs normally incurred by testing required for satellite launch qualification are significantly beyond what could be afforded by the SUNSAT development programme. The design therefore had to minimize the required testing as far as possible, and further rely on testing that could be done by sponsoring companies at no cost to the SUNSAT programme. This influenced the stiffness design requirements and strength design requirements, as described below.

Launch requirements

The launch vehicle requirements stipulate an overall minimum cantilever natural frequency, maximum allowable mass (less than 60 kg in this case), position of the centre of gravity (less than 280 mm above the separation plane) and overall dimensions (450 × 450 mm lateral, 490 mm height). Further requirements related to launch are the dimensional requirements for the PAA and the required assembly procedure (as described in the Lower Assembly Configuration paragraph).

The overall height restriction, taking the required heights of the various tray modules and sensors into account, restricts the height of the PAA-baseplate assembly to 67 mm. The baseplate and PAA further had to have the minimum weight. A specific weight limit was not imposed because the other design requirements already constrained the design.

Although stress considerations resulting from launch conditions eventually did not directly influence the baseplate design, these requirements had to be considered. The design requirements associated with stiffness and strength are discussed in more detail below.

Stiffness design requirements

One of the most stringent design requirements imposed by the launch vehicle is that of the minimum cantilevered natural frequency. While the lowest natural frequency of the complete satellite, when mounted rigidly at the separation plane, must be higher than a predetermined limit, NASA and MDA are only concerned about natural modes with frequencies below 100 Hz.

As described above, SUNSAT consists of a combination of trays bolted together to form a continuous cubical structure that has high inherent stiffness. Forces between the satellite and the launcher are transmitted through the baseplate and the PAA. The structural stiffness of the satellite assembly mounted on the launcher is therefore strongly influenced by the stiffness of the PAA and baseplate assembly.

As mentioned in the introduction, SUNSAT is scheduled for launch in the same mission as the Danish Oersted micro-satellite. The same support structure will be used for Oersted and SUNSAT. In both cases the lowest natural frequency of the complete system must be above 35 Hz to satisfy launcher requirements.[8] MDA and NASA planned to do a modal survey test with the MDA launcher support structure (PAF and support bracketry) attached to Oersted, but not with SUNSAT. If SUNSAT is designed to be stiffer than Oersted, with the same or lower mass and centre of gravity, and Oersted's modal test with the complete launcher bracketry gives satisfactory results, then SUNSAT will also be acceptable.[9] A 70 Hz cantilevered mode lowest natural frequency restriction, with SUNSAT rigidly mounted at the separation plane, was therefore placed on SUNSAT by NASA and MDA.[9] This is slightly higher than Oersted's computed lowest natural frequency, while the centre of gravity is slightly lower and the mass of SUNSAT is equal to that of Oersted.

Although this frequency is difficult to reach with a limited mass budget, the above strategy minimizes testing and analysis costs and time schedules for both SUNSAT and MDA.

Strength design requirements

The spacecraft is subjected to steady-state acceleration, vibration, and shock loads during the few minutes of launch.

Steady loads. Axial loads induced by the accelerating launch vehicle and lateral loads induced by steering and wind gusts led to the design requirement that the complete satellite must sustain 10 g accelerations of the centre of gravity simultaneously in the axial (vertical in Figure 1) and both lateral directions.[6] The lateral load factors envelope the maximum predicted flight level interface moments and shear forces.[10] Stress-related design requirements stated in terms of static accelerations are convenient to use in the finite element analysis of the complete SUNSAT structure.

The 10 g acceleration limit load factor is based on the assumption that the SUNSAT natural frequency modes do not couple with the high gain modes from the DELTA vehicle.[10] This assumption will be verified by MDA by adding the dynamic finite element model of SUNSAT (which has been correlated to the satellite structure test article used in the modal survey test) to the finite element model of the launcher support structure and recalculating the coupled natural modes of the second stage. If necessary, MDA will update the 10 g load factors to be used by SUNSAT.[10]

Critical and small components are designed to withstand 20 g accelerations simultaneously in the axial and both lateral directions.[6] This acceleration requirement is higher than the 10 g requirement for the complete structure to account for any local satellite structure modal amplification. Manual stress calculations were used for designing brackets, sensor housings, support beams, etc.

In lieu of structural static load testing, analysis with the use of a 'no test' factor of 2.0 times the maximum flight load levels (limit load factors) is an acceptable means of providing flight verification.[6] This safety factor of 2.0 is required for both main structural components and smaller components because neither will be statically tested.[10] A margin of safety for yield of above 0.65 (in other words, an additional safety factor of 1.65) is required for the complete satellite.

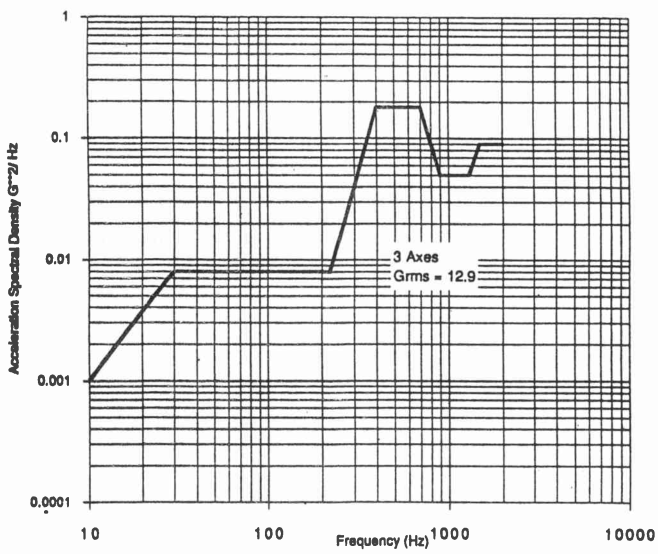

Figure 3 Prescribed flight level random vibration [6]

Vibrational loads. The significant components of the vibration loads can be classified as sinusoidal, random, and acoustic. The launch vehicle natural mode shape behaviour, steering changes, and engine ignition and shutdown normally introduce low frequency sinusoidal vibrations at the satellite-launcher interface. The random vibration environment is created by the acoustic noise generated at lift-off and during transonic flight of the launch vehicle. The maximum expected flight vibration levels are normally based on actual in-flight measurements and were provided to the SUNSAT designers for the Delta launch vehicle.[6]

The sinusoidal and random vibration environment test values are prescribed at the SUNSAT separation plane, in the form of acceleration *vs.* frequency curves. SUNSAT has to withstand a 12.9 g r.m.s. acceleration random vibration in the 10 to 2 000 Hz band for 30 s for the axial and both the lateral directions (Figure 3).[6] In vibration testing, however, industry practice is for the random vibrations to be applied for at least 60 s. In the vibration tests, the vibration is applied to the satellite by means of an electromagnetic shaker that can simulate the required acceleration distribution over the specific frequency range. SUNSAT is mounted on the shaker via a test PAA used for the modal survey test.

The fatigue loads imposed by the vibration will be present for an average time of ignited launch of about 10 minutes. With high load cycles typically not exceeding 2 000 Hz (Figure 3) and these loads occurring only a fraction of the launch time, the structure will be exposed to substantially less than 10^6 stress reversals of significant dynamic loads.

Shock loads. The maximum shock loads occur due to the abrupt fracture of the pre-loaded clamp-band (which holds the PAA and PAF together) retaining bolts by the pyrotechnic cutters during spacecraft/Delta launch vehicle separation. The shock loads are not well known, but usually do not affect the baseplate design. The ability of the baseplate to sustain these loads is therefore assessed during the mechanical launch environment testing.

Baseplate design for stiffness

The relevant design requirements are described above, particularly in the Stiffness Design Requirements paragraph.

Material selection

Aluminium was selected for both the baseplate and payload adapter fitting. Although composite materials were initially considered due to the high specific stiffness that can be achieved with some of these materials, they were not used for structural components. The selection of aluminium instead of composites was based on the following reasons:

1. The selection of aluminium was primarily based on cost reasons. Suitable aluminium is commonly available and manufacturing processes are relatively inexpensive. Space-class composite materials (that do not outgas) are not readily available in small quantities in South Africa and require more expensive manufacturing processes than aluminium. The cost constraints on a university project of this kind is such that the additional costs involved in using space class, high stiffness composite materials could not be justified.

2. Certain composite materials (e.g. carbon fibres) on the outside of the satellite are susceptible to oxidation in space due to the presence of high energy atomic oxygen. These composites have to be adequately covered to prevent this oxidation, which negates some of the mass advantages. Aluminium has adequate resistance to corrosion, both in orbit and in the atmosphere.

3. Aluminium provides better radiation shielding than low density composites. The minimum wall thickness is often determined by the radiation requirement and not only the stiffness requirement.

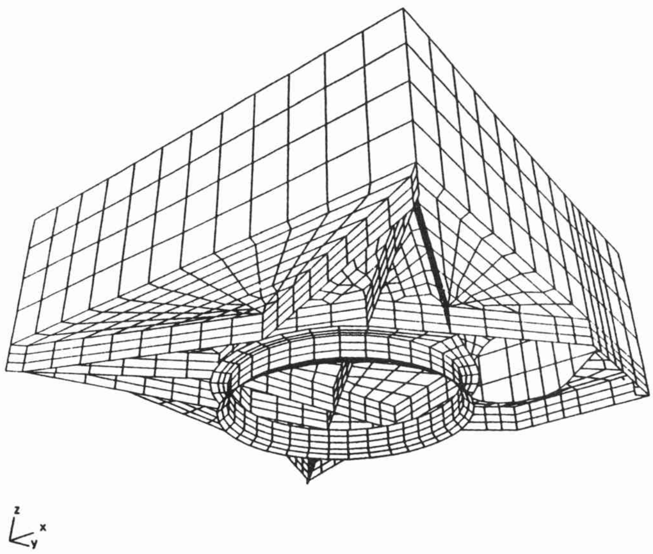

Figure 4 Finite element model of earlier baseplate configuration

Development of baseplate rib pattern and PAA interface

The original baseplate, designed to satisfy ARIANE ASAP specifications, had to be redesigned to meet the stringent stiffness requirement described above. Figure 4 shows the finite element model of one of the earlier rib arrangements that were investigated. Progressing from the first design for the ARIANE ASAP specifications, different rib placement patterns were studied to find a suitable rib pattern layout that provides the highest stiffness to mass ratio. Three factors taken into account in the arrangement of the ribs are that the load paths in the ribs should not undergo large changes in direction at the rib intersections, that the load path in any particular rib ends at a junction with another rib or a flange, and that sufficient stiffness is provided in the quadrant of the imager opening. As the total height of SUNSAT was already fixed, the maximum height that could be allocated to the baseplate was used, as that is the most effective parameter to increase stiffness while keeping mass low. It was also decided to use a bolted plate at the bottom of the ribbed structure to provide additional stiffness, as shown in Figure 5.

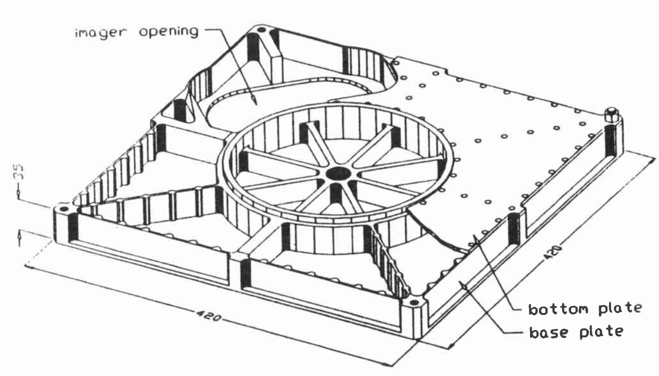

Figure 5 Final baseplate configuration

It was soon discovered that the presence of the imager opening in the baseplate was not compatible with the conventional design of a PAA, i.e. with a flange at the top that is bolted to the baseplate. No bolts could be used in the quadrant of the imager opening without obscuring the imager's view, nor are bolts allowed inside of the PAA circumference because they may not be accessible after PAA-PAF integration. A finite element analysis of the conventional flange design, without bolts in the imager opening's quadrant, revealed insufficient baseplate stiffness and excessive deflection at the bolt connections (indicating excessive stresses). It was therefore decided to use a threaded joint over the complete PAA diameter to attach the PAA to the baseplate. The absence of a flange at the top of the PAA further allowed an increase in the height of the outer ribs. This design was incorporated into the finite element model, described in the next paragraph. It exhibited a high stiffness around the whole circumference of the PAA-baseplate interface, therefore distributing the loads evenly, in contrast to concentrating loads at certain discrete connection points as in a bolted flange arrangement.

A locking ring (torqued to 1 400 Nm) will be used to preload the threaded interface. The torque is sufficient to ensure that a preload around the total circumference will be maintained during static 10 g X, Y and Z direction launch accelerations acting simultaneously.[6] A special C-spanner was designed to apply the torque and strain gauges were glued to the tool to measure the applied torque. The strain gauges were calibrated against a reference torque. Figure 2 shows the baseplate, PAA, and locking ring assembly.

Dynamic finite element modelling

The modelling of the lowest tray was added to the finite element model of the baseplate, to take the flexibility of the side walls of the bottom tray into account. The mass and inertia of the rest of SUNSAT were placed at a concentrated grid point and connected to the top corners of the bottom tray with rigid links (see Figure 6). This model was still small enough to use for structural optimizing where the NASTRAN OPTIMIZER FEM module. Each individual rib, floor and side wall thickness was iterated upon in the optimizer, with minimum baseplate structural mass as the objective function and a lowest natural frequency of 90 Hz as the constraint. A frequency of 90 Hz was used instead of 70 Hz as the flexibility of the rest of the satellite was not incorporated, which will lower the complete structure's lowest natural frequency. The optimizer converged to a top and bottom plate thickness of 4 mm spaced 35 mm apart, and rib and side wall thicknesses varying from 2.2 mm to around 16 mm. The resulting rib structure is shown in Figure 5.

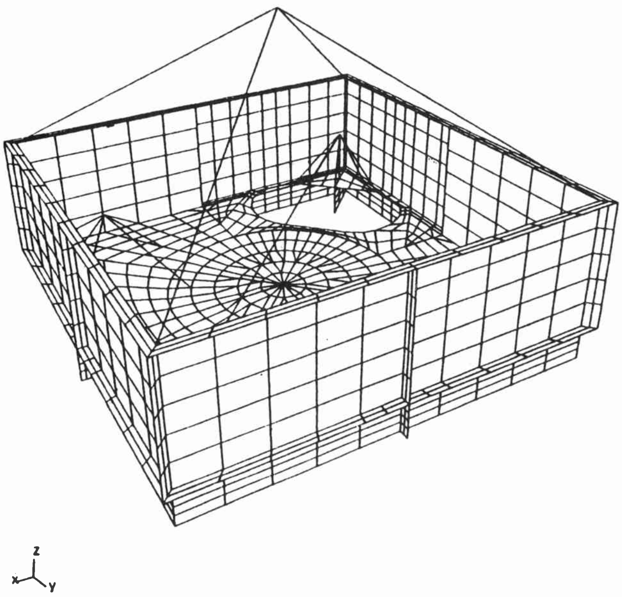

Figure 6 Finite element model of baseplate, lowest tray and concentrated mass used.

After the optimized thickness for each rib was obtained, the rest of the satellite structure was added to the finite element model to create a dynamic model of the complete satellite structure. The model represents the flight configuration of the SUNSAT satellite. The PAA, baseplate, top plate and all the computer and RF tray sides, that together form the structure, are modelled with SHELL, SOLID and BAR elements from the NASTRAN element library. The trays are interconnected with rigid constraints. The solar panels and printed circuit boards were added as SHELL and BAR elements as they have a stiffness contribution. Other specific components (e.g. the sensors, antennas, reaction wheels, etc.) are modelled as concentrated masses. The imager is modelled as a BAR element and connected to the baseplate in such a way that it provides no additional stiffness. It was ensured that the mass and centre of gravity of the complete model closely conform to that of the actual satellite hardware. The model has about 6 000 elements (and roughly the same number of grid points) and more than 30 000 degrees of freedom.

The natural frequencies of the entire satellite were calculated and studied with this finite element model. The first two modes that the model gave are the lateral bending modes at 70.0 and 70.5 Hz. The third mode is the axial mode of the top plate of the satellite at 101 Hz. Figures 7 and 8 show the first two cantilevered bending modes as calculated with the finite element model. The solar panels are removed in the figures to display the main structure better.

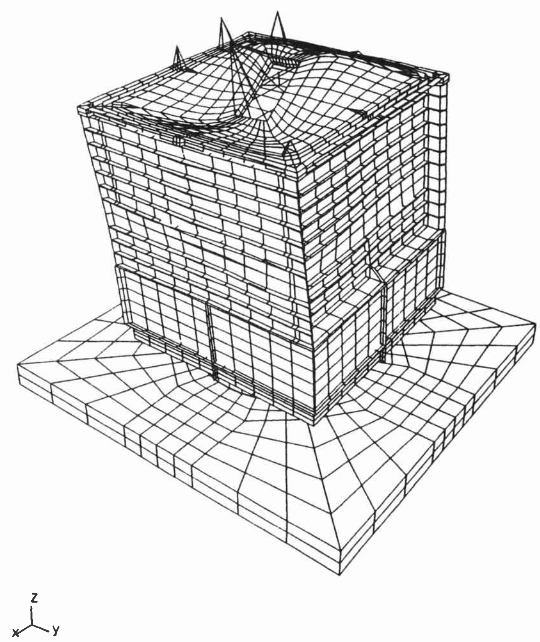

Figure 7 Computed first cantilever bending mode (solar panels removed)

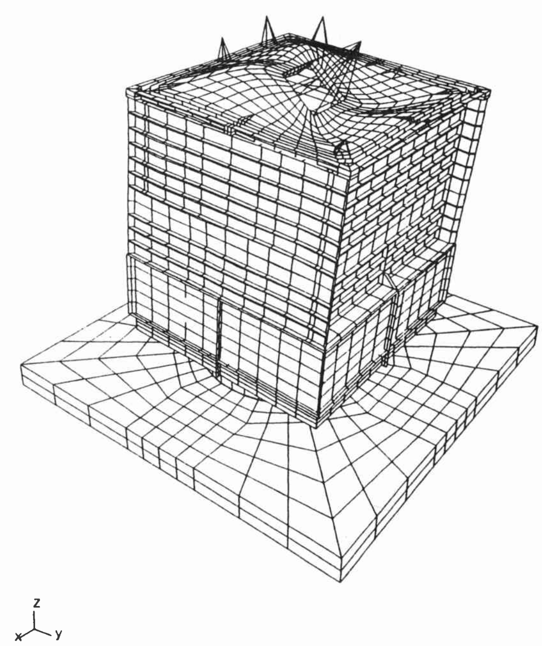

Figure 8 Computed second cantilever bending mode (solar panels removed)

Modal survey tests

The modal analysis is used to identify the natural frequencies and related modes of the structure. The modes are characteristic shapes associated with particular resonant frequencies. The shapes and frequencies are dependent on mass and stiffness properties of the complete structural system. A modal survey allows the modes to be visualized and described by identifying each resonant frequency and associated damping, mass and mode shapes. The analysis is extremely helpful in locating and correcting structural problems, such as dynamic weakness or lightly damped modes, which are major causes of vibration and fatigue failures in mechanical equipment.

In the modal survey test program, the frequency response functions at accelerometers, fixed to the satellite, are measured. These measurements are used to determine the frequency, damping and shapes of the cantilevered modes (lateral, axial and torsional) of the SUNSAT satellite about a fixed payload interface. The test results are used to perform a mathematical model correlation between the finite element model and the test article, as required by NASA.

A special test PAA was designed that can be bolted to a heavy and rigid steel plate test fixture. The test PAA is identical to the flight PAA from the separation plane upwards. A finite element model of the modal test set-up (test PAA and fixture plate) was created to check the rigidity of the test fixture. The mass and moments of inertia of the SUNSAT satellite were modeled at one grid point at the centre of gravity and connected to the bottom ring of the test PAA with rigid elements. Figure 9 shows the modal test set-up. Figure 10 shows the finite element model of the test fixture in its first natural mode. The test fixture was designed so that the lowest natural frequency with SUNSAT's mass and inertia, added at one point (centre of gravity) to the fixture, is at least 5 times higher than the same type of modal behavior (lateral bending mode) of the complete satellite model. In this way it is ensured that the addition of the test fixture finite element model to the finite element model of the satellite will not lower the natural frequencies significantly.

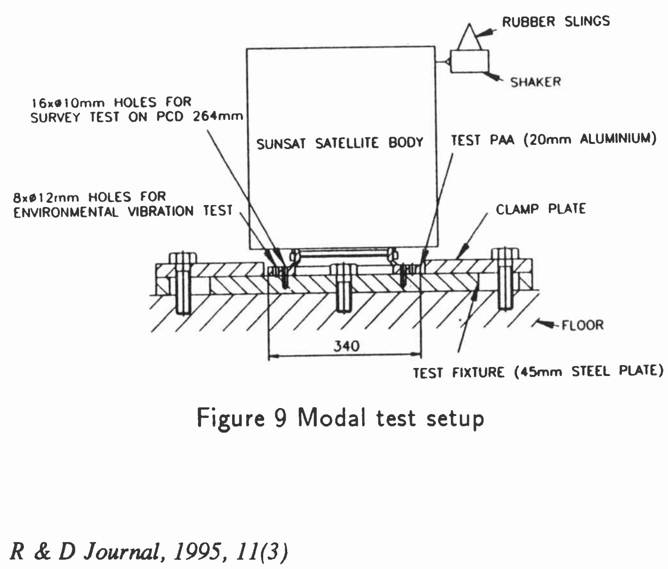

Figure 9 Modal test setup

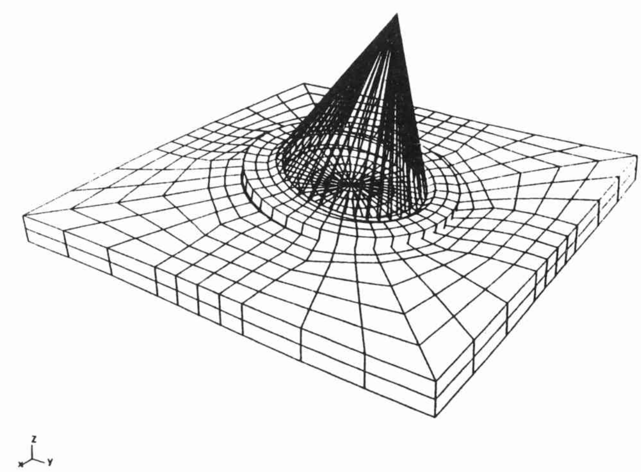

Figure 10 Finite element model of the test fixture

The first lateral bending mode of the test fixture was calculated to be 473 Hz. This is more than 6 times higher than the design mode of 70 Hz of the satellite structure rigidly supported at the separation plane. The addition of the test fixture finite element model to the finite element model of the satellite only lowers the first and second natural frequency by 0.5 Hz (70.5 to 70.0 Hz and 71.0 to 70.5 Hz). It can therefore be assumed that the test fixture provides the necessary rigidity to represent a rigid interface for the satellite at the separation plane.

Additional verification of the rigidity of the test fixture was obtained during the preliminary testing by placing accelerometers on the test fixture. Axial direction acceleration on the test fixture plate next to the test PAA flange was measured to be a fraction of the axial direction acceleration of the satellite upper corners, as predicted from the finite element model.

The test fixture finite element model was added to the dynamic finite element model of SUNSAT to form the pre-test model. The bottom grid points of the PAA were connected to the test PAA bottom ring model with rigid elements. The modelling of the solar panels was deleted and substituted with concentrated masses at the top and bottom of the satellite to represent the mass of the panels as used in the modal test.

Before the test, the selected target modes were verified by calculating the effective modal mass/inertia for each calculated frequency below 100 Hz for the pre-test model. All the modes with a modal mass/inertia to total mass/inertia ratio greater than 10% must be selected as target modes.[10] The first two bending modes have an inertia ratio of 87% and a mass ratio of 46%.

Characteristic vibrational frequencies, mode shapes, and modal damping for SUNSAT were identified in order to fulfil the test objectives and as required by NASA and MDA.[10] These parameters were established using single-point random excitation with a shaker. The shaker was placed at more than one point to insure that all the target modes were properly excited.

Table 1 shows the measured and calculated (before correlation adjustments) first two modes. A frequency response function plot of the test measurements in the lateral direction at the excitation point is provided in Figure 11. The plot shows a definite peak at the first bending mode of 65 Hz.

Table 1 Comparison of measured and calculated modes

Mode No.	Calculated frequency (Hz)	Measured frequency (Hz)	Error %	Mode shape description
1	70.0	65.0	7.7	Bending about y-axis
2	70.5	68.0	3.7	Bending about x-axis

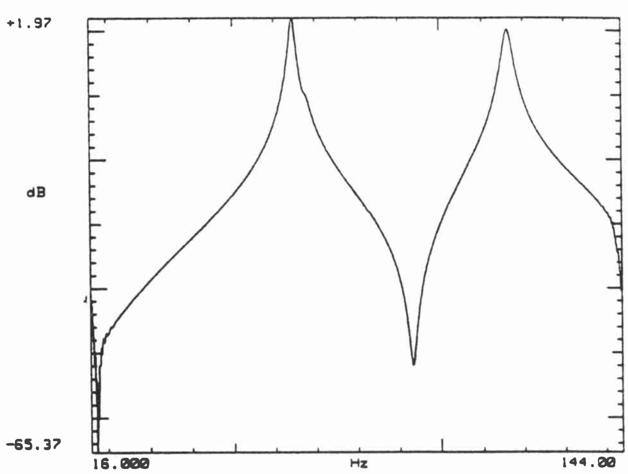

Figure 11 Frequency response function test measurements in the lateral direction at the excitation point

Test correlation and model upgrading

The main use of the modal survey test is to obtain a mathematical model of the SUNSAT satellite that is comparable in dynamic behavior to the actual flight hardware.

In the correlation procedure, the measured frequencies and mode shapes are compared to those calculated with the pre-test finite element model. This is done by obtaining a file in neutral format of the finite element model modal results. This file has the required format for the geometry, mass, stiffness matrix and modal vectors as calculated from the pre-test model and as needed by the modal comparison software (LMS CADA-X: LINK). A cross-orthogonality check and mode shape animation comparison between the measured and calculated modes (before correlation adjustments) were done.

The finite element model is accepted to represent the actual test hardware dynamic behaviour if the following correlation requirements are met for the first bending, axial and torsional modes (provided that the measured modes are less than 100 Hz):[11]

1. 5 % frequency correlation
2. cross-orthogonality check so that all the diagonal elements of the orthogonality matrix are > 0.90 and the off-diagonals are < 0.10.

Table 1 shows that mode 1 does not meet the 5% frequency correlation requirement. The cross-orthogonality check was met for the three modes below 100 Hz. Because the frequency correlation is unsatisfactory, the pre-test model will be adjusted by changing the stiffness and mass modelling in certain areas as recommended by the LINK software. The changes incorporated must always be consistent with the actual hardware.

After the necessary adjustments the correlation process is repeated to verify that the required correlation goal is met.

When the final modal correlation is successfully completed on the pre-test model, the same adjustments are incorporated into the dynamic finite element model. The dynamic model of SUNSAT then has comparable dynamic characteristics to the actual flight hardware.

Baseplate design for strength

Strength analysis

The finite element model used for the modal analysis was also used for the stress analysis of the main structural elements. A maximum Von Mises stress of 84 MPa in the main structure of SUNSAT was calculated for the 20 g (10 g times 'no flight factor' of 2) accelerations in the finite element analysis of the satellite structure. This provides a margin of safety of 4.7 relative to the 0.2% proof stress (480 MPa) of 7075 T6 aluminium that is used for the main structure. The computed safety margin therefore exceeds the value of 0.65 of the yield strength, as required by MDA.

With an ultimate tensile strength of 540 MPa, the fatigue strength of 7075 T6 aluminium is approximately 160 MPa for 10^8 stress reversals.[12] Fatigue stresses should be based on the 12.9 g r.m.s. random vibrations. Using the maximum stress value given above, and taking into account that it is based on 20 g loads, therefore gives a safety factor against fatigue failure of 3 for 10^8 stress reversals. The expected number of stress reversals, as given under the design requirements, is however less than 10^6.

During the initial phase of launch, the atmospheric air pressure in the satellite will drop quickly to space vacuum values. Although venting of enclosed sections should be adequate to prevent high pressure differences between inside and outside such volumes, a static calculation with 1 bar pressure on the inner surface of large volume sides was done to check if the surrounding structure can withstand the internal pressure in the case of insufficient venting.

Mechanical launch environmental testing

The effects of dynamic loads could be underestimated in strength calculations during main structure and component design. Spacecraft are therefore normally tested prior to launch by subjecting them to a simulated launch environment. The satellite is required to be free of any structural failures (e.g. cracks) on component level and to be electrically fully functional after completion of the test sequences.

As described under Strength Design Requirements, the satellite is subjected to steady accelerations, vibration and shock loads.

Two approaches to environmental testing are used in spacecraft design. The first one is for larger, several-of-a-kind payloads. This approach is based on a qualification and acceptance test philosophy. The first prototype or engineering model of the spacecraft is taken through formal 'qualification vibration tests' at intensities above the maximum flight vibration level (typically 3 dB for random vibration) for a duration double that of the flight.[10] Most of the hardware should be identical to that of the flight model. The test strives not only to verify functional performance, but also to produce confidence in the product by establishing design and performance margins over and above specifications. Because qualification test levels are more severe than the expected flight levels, the ability of the equipment to function properly after tests is potentially degraded. Qualification hardware is therefore not normally used for actual missions. When the design has already been qualified, acceptance testing is done on the flight hardware at normal flight levels and durations, for functional and workmanship screening.

The alternative approach is called 'protoflight level testing' and is more cost effective for one-of-a-kind payloads.[6] This is the method selected for SUNSAT. Protoflight tests are done at qualification vibration levels, but only for flight durations. The hardware is thus not overtested to the same extent as in qualification testing and can be used in a flight spacecraft. Protoflight testing therefore combines design verification and hardware screening.

Because of the complexity and cost of running an acoustic test on a satellite, random vibration tests are used for SUNSAT in lieu of acoustic tests,[6] except for the solar panels. This decision was further influenced by limited test facility availability and restricted time schedules.

For all the tests, the test article must be as close as possible to the flight configuration. All safety screws and pins of deploying mechanisms (used during assembly and transport to prevent accidental deployment) must therefore be removed during the tests. All fasteners must be torqued according to specification, but thread locking that causes permanent damage will not be used in SUNSAT tests because some of the components may need to be subsequently removed from the structure for other test programmes. At least one of the solar panels must be included in the protoflight tests. Where components are not included in the protoflight tests, the micro-climate accelerations at the component fixture points on the satellite must be measured so that protoflight tests can then be done afterwards on those components at the measured acceleration levels on a separate jig. The rest of the satellite is then not subjected to undue fatigue ageing.

The mechanical protoflight testing of SUNSAT starts with the pyrotechnic firing of the actual flight-type clamp band and attached fitting, identical to that to be used for the separation of SUNSAT from the launcher support structure. This shock load is difficult to simulate mechanically with a shaker on a complete spacecraft, without severe overtest in the low-frequency region.[6] This firing test will be done only once for protoflight screening where after the satellite will be visually inspected and tested for proper functionality. If a prototype, but not flight hardware, is qualified, two firing tests have to be performed. Possible failures that originated in the shock test will become evident in the random vibration test

The protoflight random vibration tests are done by exciting the base of the satellite at the separation plane with an electromagnetic shaker in the three axis directions for 60 s per axis.[6] The duration of 60 s is an industry standard practice for the minimum duration of an acceptance test. The overall protoflight r.m.s. random acceleration is 18.2 g (flight levels in Figure 3 plus 3 dB). After the tests, the satellite is inspected and tested for functionality again.

Finally the spacecraft is placed through the sinusoidal vibration sweep at protoflight levels (i.e.typically flight level amplitude times 1.4) up to 100 Hz.[6] Inspection and functional testing are done afterwards.

No static load testing is performed as an adequate 'no test' safety factor of 2.0 was used in the strength design.

Successful completion of the protoflight test programme verifies that the combination of design, selected materials and manufacturing processes, provides the satellite with an adequate margin of safety, and that the satellite will perform its intended functions.

Baseplate manufacturing

The baseplate was machined from a 7075 T6 grade aluminium block with original dimensions of $430 \times 430 \times 50$ mm. Welding operations were avoided because of the large variations in section thickness, the requirement to maintain tight tolerances, and the risk of trapped welding process particles coming loose in space. The bulk of the machining was done on a Beaver NC5 3-axis NC machine with a GEC Mark Century 550 controller. The controller was modified to receive cutter paths from a personal computer's parallel port instead of reading a punch tape.

Most of the machining constituted pocketing operations. CAM software was not available at the time that the baseplate's machining had to be done. Previous NC cutter paths had been generated manually or by writing special BASIC or PASCAL programs. The complexity of the baseplate's pockets, with numerous blisters to accommodate threaded holes where the bottom plate is fixed, made manual programming of the cutter paths impractical within the time constraints imposed by the launch date. The approach was therefore taken to generate the cutter paths using an existing 2-D CAD system, plot these paths to a plot file in HPGL format, and convert the 'plots' to G-codes by means of a program written for this purpose.

The definition of the cutter paths for the pocketing operations was efficiently performed on the CAD system by generating offset curves of the pocket outlines (offset at the cutter radius) and using hatching to define cutter paths for material removal in the interior of the pocket. Lines defining suitable cutter movements from one hatching line to the next were added individually. The resulting cutter paths, excluding depth information, were plotted to files in HPGL format, using pen numbers to distinguish between the pocket outline cut and the interior material removal.

The HPGL-to-G-codes program read the line segments from the plot file, sorted the line segments to ensure continuous cuts where possible, and allowed the user to specify cutting depths and increments. HPGL commands do not include circular interpolation, with the result that arcs are represented by numerous short straight line segments in the plot file. To improve the surface quality of arcs, the program searches for circular arcs and estimates the position of the centre of each arc, using a two-dimensional steepest gradient search. It allows the user to update the centre point coordinates and to further instruct the program whether to convert any arc from straight lines to circular interpolation, or to retain the straight lines.

Although this approach in generating cutter paths was developed due to time and financial constraints in the SUNSAT program and is unconventional, subsequent experience indicates that, for many pocketing operations, it is more productive than transferring CAD data to CAM software and then using the CAM software to generate the cutter paths.

The cutter paths were verified beforehand by cutting samples in wood.

Conclusions

The design, testing procedure and manufacturing of the SUNSAT micro-satellite baseplate and mounting ring were described. The wide range of requirements that the design has to satisfy were discussed, with particular attention to requirements relating to stiffness and strength. The process of experimental verification of the modal analysis and strength design were described.

Through the combination of engineering judgement, finite element analysis techniques and low cost NC-machine programming, the baseplate and mounting ring of SUNSAT were designed and manufactured to meet the stated design requirements. This was accomplished within the allowable cost and timescales. Analyses and tests verified that the stiffness and strength design requirements were met. The final mass of the baseplate is 5,7 kg and that of the PAA 1,3 kg.

References

[1] Schoonwinkel A & Milne GW. Adaption of the SUNSAT Micro Satellite for the Argos/P91-1 Delta Mission. *Proc. IEEE/SAIEE SS&C-94*, University of Stellenbosch, 1994.

[2] Horais BJ. International Activities in Small Satellites. *6th Annual AIAA/USU Small Satellite Conference*, 1993.

[3] Hatleid JE & Sterling DE. *A Survey of Small Spacecraft in Commercial Constellations.* Motorola Inc., McLean, VA, 1992.

[4] Sweeting MN. UoSAT Microsatellites and Minisatellites for Affordable Access to Space. *Proc. IEEE/SAIEE SS&C-94*, University of Stellenbosch, Stellenbosch, 1994.

[5] Schuster HR & Basson AH. Aspects of SUNSAT Main Structure Design and Manufacturing. *R&D Journal*, 1995, **11**, 21–28.

[6] Delta Launch Vehicle Secondary Payload Planner's Guide for NASA Missions. Orbital Launch Services Project, National Aeronautics and Space Administration, Goddard Space Flight Center, Maryland, USA, 1992.

[7] Griffin MD & French JR. Space Vehicle Design. *AIAA*, Washington, DC, 1991.

[8] Johnson B. Oersted Support Structure Design and Dynamic Model Review. *Oersted Support Review*, 1994.

[9] SUNSAT Modal Testing Meeting Minutes. McDonnell Douglas Aerospace - West, California, USA, 1994.

[10] SUNSAT Integration Meeting Minutes. McDonnell Douglas Aerospace, Space Transportation Division, Huntington Beach, California, USA, 1994.

[11] Helin AS. *Dynamic Model Development Guidelines for Secondary Payloads on Delta 11 Air Force Launch Vehicles.* McDonnell Douglas Aerospace, Space Transportation Division, Huntington Beach, California, USA, 1992.

[12] Shigley JE. *Mechanical Engineering Design*, 1st metric edn. *McGraw-Hill, New York, 1986.*